JOURNAL OF MATERIALS SCIENCE 19 (1984) 3692–3701

The thermal shock of ß-alumina

J. R. G. EVANS, R. STEVENS
Department of Ceramics, Houldsworth School of Applied Science, University of Leeds, Leeds, UK

S. R. TAN
Chloride Silent Power Ltd, Runcorn, Cheshire, UK

The thermal shock of sodium β-alumina with relative densities from 60 to 98% theoretical has been investigated over the temperature range 150 to 700° C by quenching into water. The samples were ring segments cut from electrolyte tubes and were subsequently tested in both compression and tension. For relative densities of 75% and below the thermal shock damage was typical of stable crack growth and a steady decline in strength with sintering temperature was observed. For relative densities of 95% and above, thermal shock causes unstable crack growth and a critical value of ΔT was observed in the range 170 to 250° C depending on initial strength. From the linear relationship between observed ΔT_c and the thermal shock resistance parameter, R, it was concluded that the rapid heat transfer during quenching was nucleate water boiling and that cooling from ~ 110° C to 0° C was not responsible for damage. The fracture stress after thermal shock above ΔT_c was consistent and showed little dependence on initial strength for relative densities $\geqslant$ 95%. However, the fractional reduction in strength was related to the damage resistance parameter R'''. An estimate of the energy expended in fracture has been made, based on microscopic observation and compared with estimates of the stored strain energy due to thermal stresses.

1. Introduction

Sodium β-alumina is currently being exploited in the development of the sodium sulphur battery which is intended for application in vehicle propulsion and for load levelling in the electricity supply industry. For this purpose β-alumina is fabricated by continuous zone sintering into thin walled tubes. During the fabrication route these tubes may become subject to rapid changes in temperature as high production speeds are demanded. This work presents a basic study of the thermal shock behaviour of β-alumina in a range of partially and fully sintered states.

The most exacting condition for thermal shock damage is cooling of the surface, presenting tensile stresses to the surface flaws. Water quenching similarly provides a severe cooling condition and has been used here to study the thermal shock of β-alumina samples in the form of semicircular ring segments cut from manufactured electrolyte tubes. The method of investigation used was to compare the strengths of unshocked samples tested in both compression and tension with the strengths of similar samples which had been subject to a water quench from varying temperatures. The initial strength is a function of pre-existing surface flaws and the strength after thermal shock is used as a measure of the extent to which these flaws have been extended under the influence of tensile thermal stress generated in the surface.

The material examined was identical to that previously described in a study of the sintering of β-alumina [1]. The maximum strength was obtained for a sintering temperature of 1600° C and the strength associated with flaws on the internal surface was generally up to 20% higher than that of the outer surface of tubes. Thus using the "C"-ring test the thermal shock behaviour of both surfaces for each sintering temperature could be studied.

0022–2461/84 $03.00 + .12

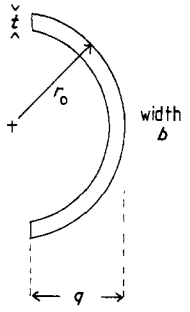

Figure 1 Dimensions of ring segments.

2. Experimental techniques

Tubes were fabricated by isostatic pressing of spray dried powders, having a composition after prefiring of 8.75% Na_2O, 1% MgO, 0.5% Li_2O, balance Al_2O_3. Sintering was performed in an induction-heated zone-sintering furnace with a rotating alumina work tube. Details of the thermal conditions, in particular the temperature gradients, are given elsewhere [1]. Samples were variously sintered at peak furnace temperatures in the range 1400 to 1710° C.

After fabrication, rings 10 mm wide were cut from the tubes with a diamond-impregnated cutting blade using an organic coolant and slow feed rate, to minimize damage. The rings were further cut into semicircular segments using a thin (0.5 mm) diamond-impregnated wheel. The dimensions of each ring segment were recorded as shown in Fig. 1. The thickness was measured at the centre of each of the segments.

Thermal shock testing was performed using the apparatus described in Fig. 2. Although previous work [2] had shown that there was little systematic variation in strength along the length of the tubes, samples were selected at intervals of 150 mm for each test temperature. They were then raised to the desired quenching temperature in a stainless steel wire basket, the maximum rate of heating being 30° C min^{-1}, with the hot zone at 700° C. When the sample was positioned in the hot zone a microswitch disconnected the motor and a soaking time of 15 min was allowed for temperature equilibration. The lower furnace door was then opened and the basket immediately released and allowed to fall into water cooled with ice to 0° C. After drying in acetone and air, the ring segments were tested in compression and tension in an Instron testing machine with a crosshead speed of 0.1 mm min^{-1}. The expressions for the maximum stress in the outermost fibres (σ) are approximated [3] by:

$$\sigma = \frac{P}{bt} K \tag{1}$$

where

$$K_{\text{compression}} = \frac{6(q - t/2)}{t} - 3 \tag{2}$$

$$K_{\text{tension}} = \frac{6(q - t/2 - d)}{t} + 3, \tag{3}$$

for $r_0/r_1 = 1.10$, where d is the correction for the displacement of the loading axis from the diameter when using the tensile testing grips [3]. The other dimensions (in mm) are given in Fig. 1, and give values for σ in MPa.

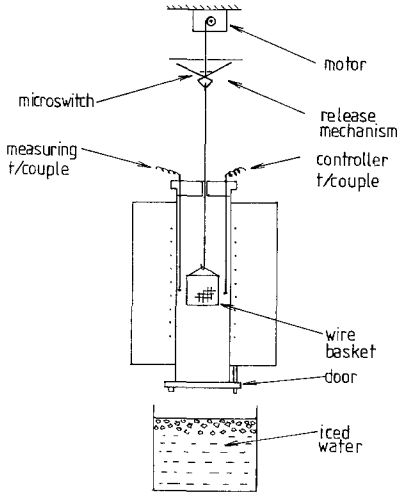

Figure 2 Thermal shock apparatus.

3. Results and discussion

3.1. Resistance to thermal shock

Figs. 3 to 7 show the thermal shock behaviour of the β-alumina samples prepared over a range of sintering temperatures from 1400 to 1710° C. The fracture strengths, σ_f, for "C"-ring tests in compression and tension are plotted as a function of the temperature to which the samples were heated before being plunged into water held at 0° C. For specimens sintered at temperatures in the range 1400 to 1500° C, corresponding to porosity levels from 37 to 25%, the thermal shock curves show a steady decline in strength with increasing severity of quench. This behaviour illustrates the quasi-static crack propagation typical of porous ceramics [4]. The effect of the porosity tends to be to

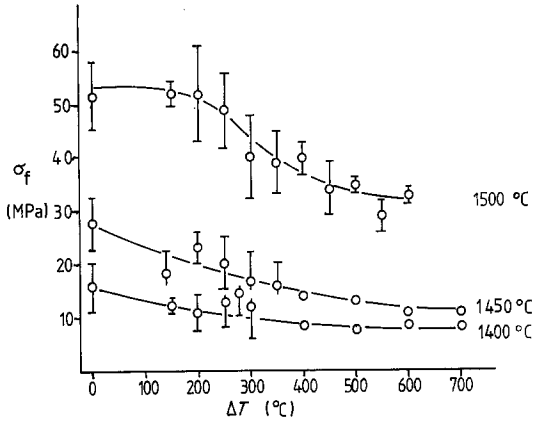

Figure 3 Thermal shock curve for β-alumina sintered at 1400, 1450 and 1500° C (outer surface tested).

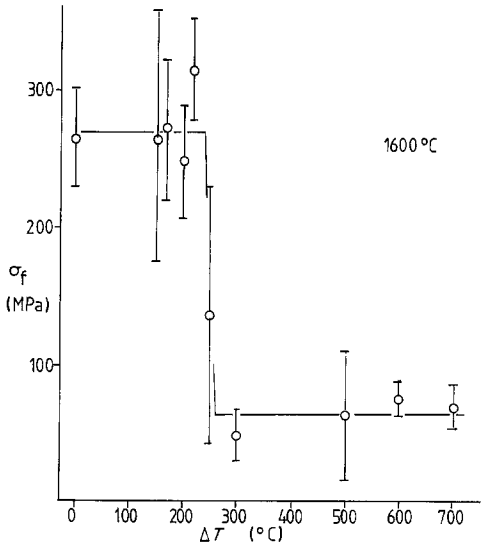

Figure 5 Thermal shock curve for β-alumina sintered at 1600° C (inner surface tested).

reduce the resistance to thermal shock by reducing the strength and thermal conductivity [5], but to improve the resistance to damage. The effect of porosity on strain at failure σ_f/E [1] and on strength is such as to reduce the elastic energy stored at fracture and hence the total area of crack propagation [6]. A further effect is that of crack blunting due to the interaction with pores which results in quasi-static crack growth during the thermal shock process.

For sintering temperatures of 1550° C and above, corresponding to porosity levels of $\leqslant 5\%$, crack propagation during shock is unstable and a critical thermal shock temperature, $\Delta T_c'$, was used thermal shock damage, ΔT_c, was observed. Below ΔT_c no reduction in strength occurred and above ΔT_c the strength remained constant until a higher critical thermal shock temperature, $\Delta T_c'$, was used whereupon a steady decline in strength develops [4]. The value of $\Delta T_c'$ is not clearly defined for most of the experiments reported here; emphasis is placed upon the determination of ΔT_c, which marks the onset of damage. The parameters which define the thermal shock behaviour of brittle solids have been extensively investigated [4, 7, 8] and their evaluation requires a knowledge of the thermal and mechanical properties of the material. Relevant properties of the β-alumina samples used are listed in Table I. There is some difficulty in knowing accurately the value for the heat transfer coefficient for a water quench which can vary from 10^4 to $10^5\,W\,m^{-2}\,K^{-1}$ [9] depending on the

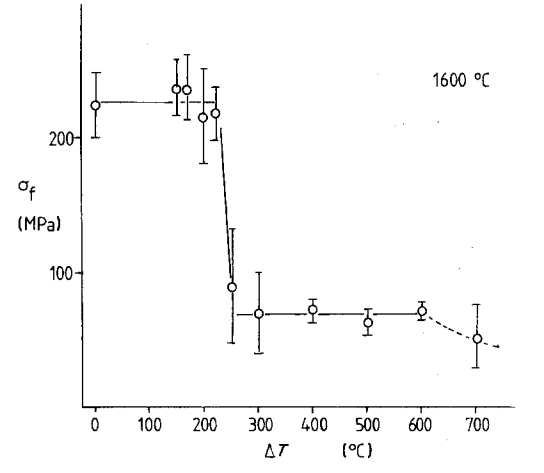

Figure 4 Thermal shock curve for β-alumina sintered at 1600° C (outer surface tested).

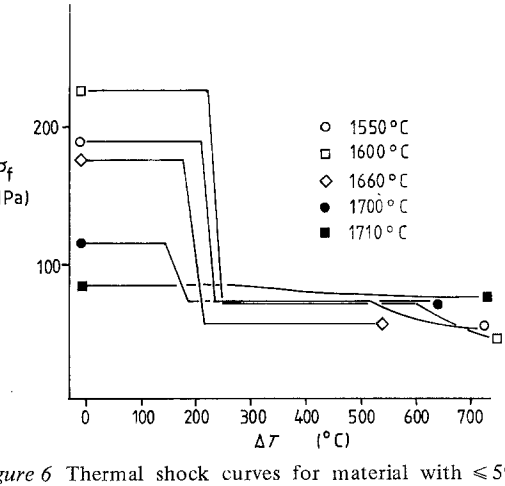

Figure 6 Thermal shock curves for material with $\leqslant 5\%$ porosity (outer surface tested).

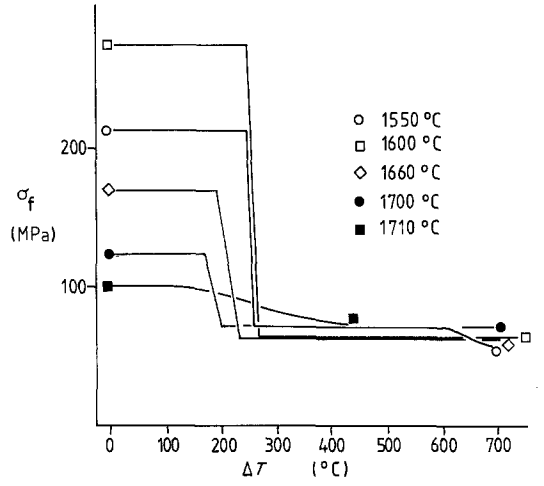

Figure 7 Thermal shock curves for material with ⩽5% porosity (inner surface tested).

type of boiling. The value in Table I is that preferred by Davidge and Tappin [10] and is used to give an estimate of the Biot number $\beta = r_m h/k = 30$. Because the thermal conductivity of β-alumina in an order of magnitude below that of pure alumina, instantaneous quench conditions can be more easily approximated in practice. Thus using the data for an infinite flat plate given by Kingery [7] the non-dimensional stress factor, A, in Equation 4, takes the value 0.7 at $\beta = 20$. The tensile thermal stress at the surface of the plate is then given by:

$$\sigma = AE\alpha\Delta T/1 - \nu \quad (4)$$

where E is Young's modulus, α is the linear thermal expansion coefficient, ν is Poisson's ratio, and ΔT is the temperature difference between the inside of the body and the surface. Using values of $E = 197$ GPa and $\nu = 0.27$ [12] for β-alumina, Equation 4 becomes:

$$\sigma = 1.51 \times 10^6 \Delta T, \quad (5)$$

or, equating σ with the failure stress of the as-fabricated material, σ_i, ΔT is then an estimate of the critical temperature difference needed to produce thermal shock damage ΔT_c:

$$\Delta T_c = 0.66\sigma_i \quad (6)$$

where the units of σ_i are MPa.

However, σ_f measured on unshocked "C"-rings at low strain rates in air may not be equivalent to the failure stress of the same material under thermal shock conditions where different environmental conditions might prevail. The strain rate in water-quench conditions is much higher than for mechanical testing at low crosshead speeds but if any environmental effect is present it cannot be assessed at present. The values of ΔT_c and σ_i determined for internal and external surfaces of tubes sintered at 1550° C and above (Table II) were plotted in Fig. 8. A least squares fit for the resulting straight line gives:

$$\Delta T_c = 0.44\sigma_i + 125 \quad (\sigma_i \text{ in MPa}). \quad (7)$$

Fig. 8 offers a useful way of predicting thermal shock resistance from a knowledge of the initial strength only. It is noteworthy that it includes data for a wide range of strengths resulting from quite different flaw types [1]. The undersintered material prepared at 1550° C included regions of low density (pore clusters) originating from the packing of large powder agglomerates while the oversintered samples (1700° C) are weakened by

TABLE I Property values used in thermal shock resistance tests

Half thickness r_m	8.5×10^{-4} m
Heat transfer coefficient, h (water quench)	100 kW m^{-2} K^{-1} [11]
Thermal conductivity, k	3.6 W m^{-1} K^{-1} at 25° C 2.9 W m^{-1} K^{-1} at 445°C [12]
Coefficient of linear expansion	8×10^{-6} K^{-1} [13]
Biot modulus	30

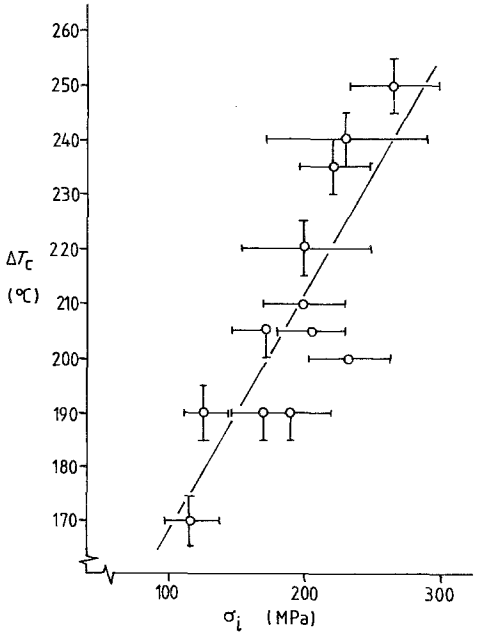

Figure 8 ΔT_c as a function of initial strength for β-alumina with ⩽5% porosity.

TABLE II Observed T_c, initial strength and thermal shock resistance parameter R

Sintering Temp. (° C)	C/T*	$\sigma_i \pm$ S.D. (MPa)	(n)	E (GPa)	R (° C)	$\Delta T_c \pm 5$ (° C)
1550	C	200 ± 47	(12)	150	174	220
1550	T	231 ± 61	(10)	150	201	240
1600	C	223 ± 23	(14)	173	168	235
1600	T	266 ± 36	(12)	173	199	250
1660	C	169 ± 27	(10)	197	113	205
1660	T	171 ± 25	(9)	197	112	190
1700	C	117 ± 21	(4)	197	77	170
1700	T	127 ± 13	(4)	197	84	190
1660†	C	192 ± 28	(20)	–	–	190
1660†	T	213 ± 27	(20)	–	–	205
1660‡	C	194 ± 39	(30)	–	–	210
1660‡	T	232 ± 34	(30)	–	–	200

*C, outer surface under test; T, inner surface under test.
†Material fired in pilot plant furnace unannealed.
‡Material fired in pilot plant furnace annealed 1400° C, 3 h.
n: number of measurements.

cleavage flaws occurring on the basal planes of large connected grains [1].

Since all the data in Fig. 8 are for relative densities greater than 95%, the difference in thermal conductivity is not expected to alter the Biot number sufficiently to have an effect on the value of A in Equation 4. The value of α would not be expected to change but the elastic modulus is affected and values obtained by a sonic resonance technique are given in Table II. From these data the thermal shock resistance parameter, R, is calculated and compared with ΔT_c deduced from the strength–temperature graphs. These are plotted in Fig. 9 where the least squares fit for the β-alumina results takes the form:

$$\Delta T_c = 0.54R + 137 \quad (8)$$

In both Equations 7 and 8, there is an indication that ΔT_c includes a constant term uninfluenced by the mechanical property variables. It should be remembered that ΔT is the temperature to which the samples were raised before quenching into water at 0° C. Because the quenching temperatures are well above the boiling point of water (ΔT_c lies in the range 170 to 250° C), it is thought that the boiling water interface is the predominant rate-controlling path for high heat transfer which produces damage. Subsequent cooling to 0° C is too slow to cause further damage ($\beta \ll 30$ for $\Delta T <$ 100° C). This is supported by studies of water-quenching effects by high speed photography which shows that boiling is the cause of high heat transfer rates at temperatures above ~180° C [14]. At very high temperatures an insulating

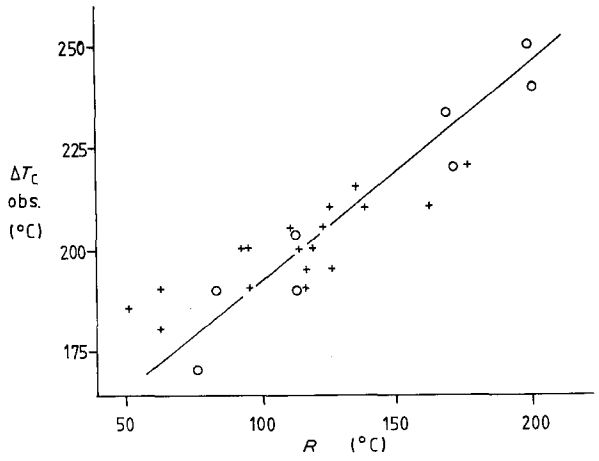

Figure 9 Thermal shock resistance parameter, R, as a function of observed ΔT_c for β-alumina (○) compared with values for α-alumina (×) from [10]. (Least squares fit for β-alumina: solid line.)

steam barrier is expected to reduce heat transfer [9].

Fig. 9 also includes data for a range of α-aluminas taken from Davidge and Tappin [10] for comparison. The authors used $R/3$ to compensate for environmental effects in water quenching but in Fig. 9 this arbitrary factor is omitted and the least squares fit gives:

$$\Delta T_c = 0.28R + 169. \quad (9)$$

The difference in gradient of the equation can be attributed to difficulties in evaluating the heat transfer coefficient, to the cylindrical α-alumina samples and to possible environmental effects.

3.2. Resistance to damage

The strength of the material after thermal shock treatment above ΔT_c is a measure of the extent to which pre-existing surface flaws have been enlarged by biaxial tensile thermal stresses originating from the difference in temperature between the inside of the body and its surface. The existence of crack instability between the two critical temperature differences ΔT_c and $\Delta T_c'$ gives a clearly defined as-shocked strength, σ_s, and the average value of $\bar{\sigma}_s$ for all the quench conditions between ΔT_c and $\Delta T_c'$ is shown in Table III and plotted against initial strength σ_i (Fig. 10). This shows that for porosity levels below 5%, that is for specimens having an initial strength σ_i greater than 80 MPa, the as-shocked strengths are remarkably constant and exhibit little dependence on initial strength.

TABLE III Average strength after thermal shock, $\bar{\sigma}_s$, and initial strength σ_i

Sintering temperature (° C)	C/T*	σ_i (MPa)	$\bar{\sigma}_s \pm$ S.D. (MPa)
1400	C	15.7	7.9 ± 2.3
1450	C	27.5	11.9 ± 1.5
1500	C	51.5	32 ± 4.3
1550	C	200	74 ± 15
1550	T	231	68 ± 10
1600	C	223	69 ± 15
1600	T	266	61 ± 22
1660	C	168	57 ± 8
1660	T	171	64 ± 10
1700	C	116	71 ± 4
1700	T	127	68 ± 19
1710	C	92	72 ± 8
1710	T	84	75 ± 10

*C, tested in compression (outer surface under test); T, tested in tension (inner surface under test).

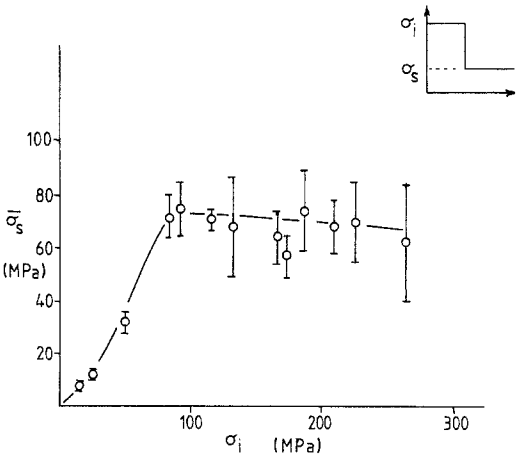

Figure 10 Average strength after thermal shock ($\Delta T > \Delta T_c$) plotted against initial strength.

The reduction in strength due to thermal shock expressed as a percentage of the initial strength was plotted in the form used by Morgan [17] for thermal shock of clay bodies and referred to by Hasselman [6] as evidence for the parabolic relation between damage and initial strength:

$$\sigma_i = \sigma_{max}\left(\frac{P}{100}\right)^{1/2}, \quad (10)$$

where σ_{max} was the maximum recorded initial strength and P was the reduction expressed as a percentage. Using data for the 400° C quench, Table IV shows these data which are plotted in Fig. 11. Although the parabolic relationship is not well illustrated, the damage in samples known to have

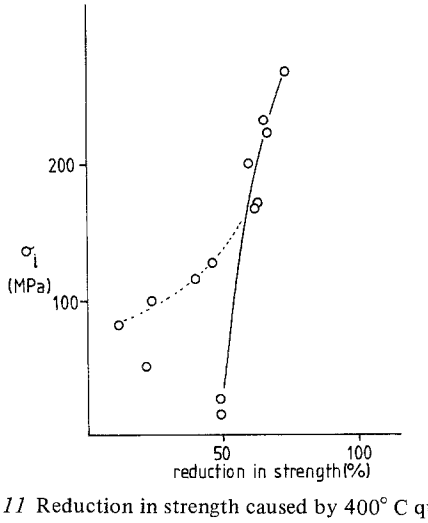

Figure 11 Reduction in strength caused by 400° C quench plotted against initial strength in the manner of [17]. Dashed curve: large grain defects.

TABLE IV Initial and shocked strengths for 400° C quench

Sintering temp (° C)	C/T*	σ_i (MPa)	σ_s (MPa)	$P = \frac{\sigma_i - \sigma_s}{\sigma_i}$ (%)
1400	C	15.7	8	49
1450	C	27.5	14	49
1500	C	51.5	40	22
1550	C	200	80	60
1550	T	231	78	66
1600	C	223	73	67
1600	T	266	70	74
1660	C	169	63	63
1660	T	171	61	64
1700	C	116	70†	40
1700	T	127	69†	46
1710	C	82	73	11
1710	T	100	76	24

*C, samples tested in compression (outer surface under test); T, samples tested in tension (inner surface under test).
†$\Delta T = 450°$ C.

large grain defects [3] lies on a different locus (dashed curve) to that for samples where the strength-controlling defects are large regions of porosity. The data point which lies off the curve is for the 1500° C sintering temperature where $\Delta T = 400°$ C gives an unusually high strength (cf. $\bar{\sigma}_s$; Table III). The difference in behaviour is less clear if the absolute loss in strength $\sigma_i - \sigma_s$ is plotted against σ_i (Fig. 12); here the dashed line refers to material with large grain defects and the solid line to material with pore clusters.

Using the calibration for crack depth as a function of strength [3], the strength after thermal shock, σ_s, in Fig. 10 corresponds to crack depths in the region of 500 μm. For the case of an infinite plate, Manson and Smith [11] indicate that the depth of tensile stress at the time of maximum probability of failure (which is greater than the time of maximum tensile surface stress) is of the order $0.3r_m$. Thus crack depths after severe thermal shock are approximately twice the depth of the expected tensile stresses at the moment of maximum probability of failure.

The thermal shock damage resistance parameter

$$R''' = \frac{E}{\sigma_i^2(1-\nu)} \tag{11}$$

was calculated for all the β-alumina materials and compared with the reduction in strength for a 400° C quench (Table V). With the exception of

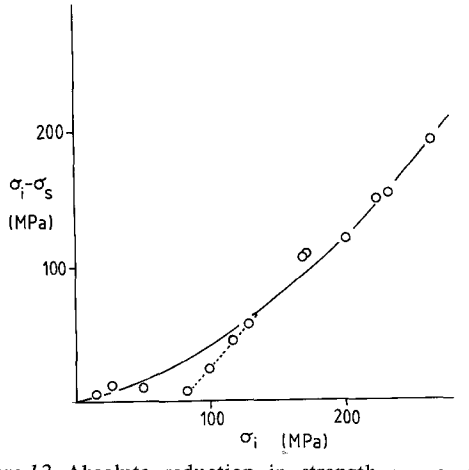

Figure 12 Absolute reduction in strength $\sigma_i - \sigma_s$ as a function of initial strength, σ_i, for 400° C quench. Dashed curve: large grain defects.

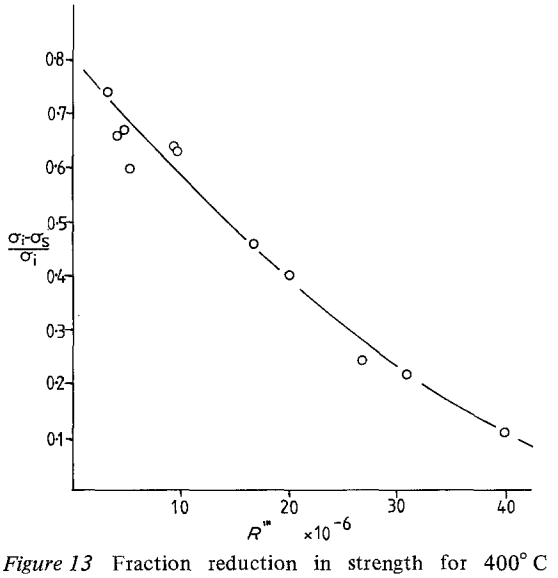

Figure 13 Fraction reduction in strength for 400° C quench compared with damage resistance parameter R'''.

TABLE V Fractional reduction in strength compared with damage resistance parameter R''' for the 400° C quench

Sintering temp. (° C)	C/T	E (10^{11} Pa)	$\frac{\sigma_i - \sigma_s}{\sigma_i}$	$R''' = \frac{E}{\sigma_i^2(1-\nu)} \times 10^{-6}$
1400	C	0.28	0.49	156
1450	C	0.36	0.49	65
1500	C	0.63	0.22	31
1550	C	1.50	0.60	5.1
1550	T	1.50	0.66	3.9
1600	C	1.73	0.67	4.8
1600	T	1.73	0.74	3.4
1660	C	1.97	0.63	9.5
1660	T	1.97	0.64	9.2
1700	C	1.97	0.40	2.0
1700	T	1.97	0.46	16.7
1710	C	1.97	0.11	40
1710	T	1.97	0.24	27

the data for 1400 and 1450° C samples which have extreme values of R''', the data were plotted in Fig. 13. The decrease in $\sigma_i - \sigma_s/\sigma_i$ with R''' suggests that this parameter is suitable for evaluating the thermal shock damage of β-alumina.

In the energy balance approach to thermal shock damage, the elastic energy stored in the body at fracture is equated with the product of the total area of cracks and the effective surface energy of fracture, γ_{eff} [4, 6]. Treating the "C"-ring samples as flat plates ($r_2/r_1 = 1:1$), the stored elastic energy at fracture per unit area on one side only, equating the fracture stress in thermal shock with that measured in air, σ_i, is:

$$W = \frac{0.3 r_m \sigma_i^2 (1-\nu)}{2E} = \frac{0.15 r_m \sigma_i^2 (1-\nu)}{E}, \quad (12)$$

where r_m is the plate half thickness. The factor 0.3 arises because it is only the contribution from tensile stresses that is considered to generate damage and for a Biot number of 30 the depth of tensile stresses from the outer surface is $\sim 0.3 r_m$ at the time when there is a maximum likelihood of rupture [11]. If the average crack depth after thermal shock is $\overline{C_s}$ and the crack length per unit area is l, then the total surface energy of the crack is

$$U = 2\overline{C_s} l \gamma_{eff}. \quad (13)$$

The value of $\overline{C_s}$ was estimated from the maximum crack depth from a knowledge of the critical stress intensity factor [3], i.e. 2.9 MPa $m^{1/2}$. This approximation tends to overestimate U. The crack length l was measured using optical micrographs by image analysis*. The lowest value of γ_{eff} was used [2]. In this way values of U and W are tabulated in Table VI. For samples without large grains (1500 and 1600° C) the maximum available strain energy is consumed for the high temperature quench and the agreement between U and W is reasonable considering that $\overline{C_s}$ is overestimated by using the maximum crack depth, C_s, from fracture stress and that the true value of the fracture stress in thermal shock is only approximated by σ_i.

TABLE VI Stored elastic energy, W, and crack surface energy, U, for external surfaces

Sintering temp. (° C)	ΔT (° C)	C_s (μm)	L (m^{-1})	U (J m^{-2})	W (J m^{-2})
1550	400	420	510	5	25
	700	520	1810	21	
1600	300	470	570	6	27
	400	440	2100	20	
	500	570	3410	43	
	600	470	3360	35	
	700	600	3000	40	

*Kontron (West Germany).

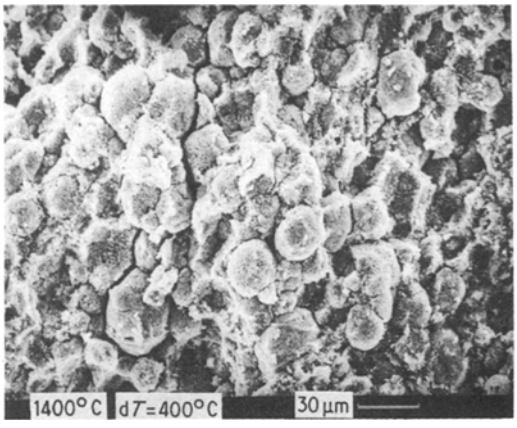

Figure 14 SEM fracture surface of sample sintered at 1400° C after thermal shock at 400° C.

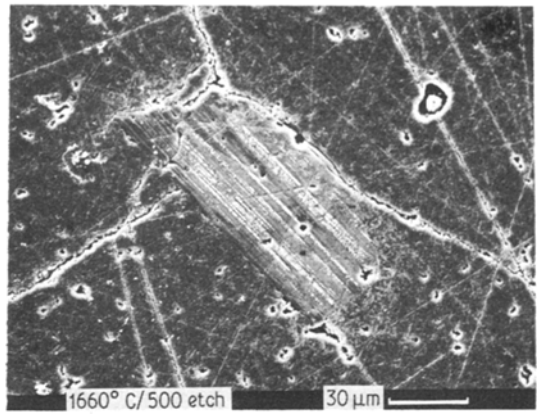

Figure 16 SEM polished and etched (hot H_3PO_4) section of 1660° C material after 500° C quench.

For high porosity samples (sintering temperature $< 1500°$ C) the thermal shock damage is associated with separation of powder agglomerates and is shown on fracture surfaces in Fig. 14. The thermal shock cracks appear on the outer surface (Fig. 15) of unfractured samples. For higher density material the cracks are revealed by etching polished sections. Fig. 16 shows thermal shock cracks in several directions in a large β-alumina grain (sintering temperature 1660° C).

Defects normally associated with the initiation of fracture in mechanical loading may not always play such a crucial role in thermal shock damage. Fig. 17 shows a crack junction where a crack has passed within 5 μm of a large pore apparently uninfluenced by it. Fig. 18 shows the similar situation for a large β-alumina grain adjacent to a crack junction.

4. Conclusions

The thermal shock of β-alumina with a range of densities produced by variation in sintering conditions has been investigated by quenching into water at 0° C. For high porosity material, low initial strength is accompanied by low thermal shock resistance and good resistance to damage by stable crack growth. For low porosity levels $\leqslant 5\%$, a clearly defined critical temperature difference ΔT for onset of thermal shock damage was observed and was found to be a function of initial strength. A good correlation between the resistance parameter R and measured ΔT_c was found over a range of materials where fracture initiated from flaws situated in large grains and also in pore clusters.

The extent of damage indicated by the drop in strength at ΔT_c was found to correlate with the

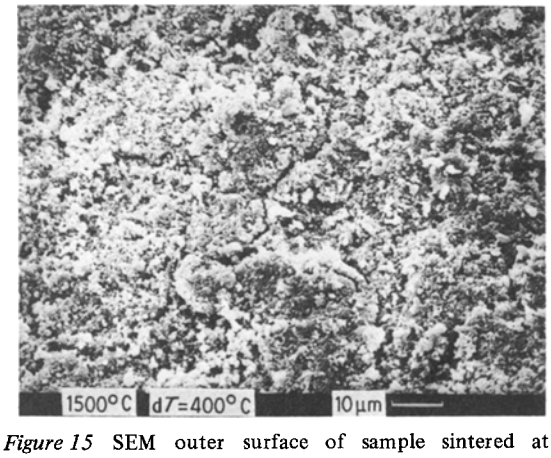

Figure 15 SEM outer surface of sample sintered at 1500° C and quenched from 400° C.

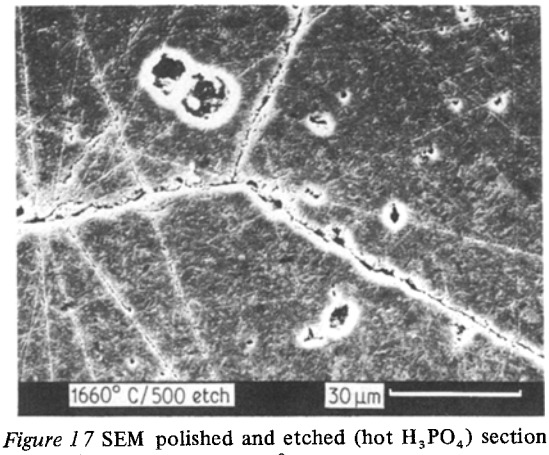

Figure 17 SEM polished and etched (hot H_3PO_4) section of 1660° C material after 500° C quench.

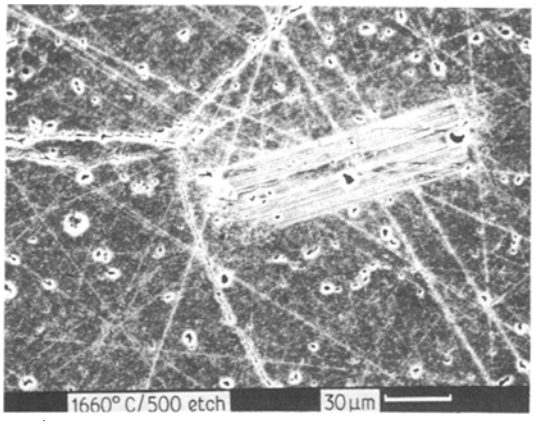

Figure 18 SEM polished and etched (hot H_3PO_4) section of 1660° C material after 500° C quench.

damage resistance parameter R''', but the absolute value of the as-shocked strength did not vary greatly for the whole range of low porosity materials. The reduction in strength was generally lower for samples with large grain critical defects than for those with pore cluster defects. A comparison of estimates of energy expended in crack growth with stored strain energy due to quenching gave reasonable agreement for material without large grains.

Acknowledgements

The authors thank S.E.R.C. for research support and Chloride Silent Power Ltd for their help.

References

1. J. R. G. EVANS and R. STEVENS, *Trans. Brit. Ceram. Soc.* 83 (1984) 43.
2. S. R. TAN, G. J. MAY, J. R. McLAREN, G. TAPPIN and R. W. DAVIDGE, *Trans. J. Brit. Ceram. Soc.* 79 (1980) 120.
3. J. R. G. EVANS and R. STEVENS, *Trans. Brit. Ceram. Soc.* 83 (1984) 14.
4. D. P. H. HASSELMAN, *J. Amer. Ceram. Soc.* 52 (1969) 600.
5. R. L. COBLE and W. D. KINGERY, *ibid.* 38 (1955) 33.
6. D. P. H. HASSELMAN, *ibid.* 46 (1963) 535.
7. W. D. KINGERY, *ibid.* 38 (1955) 3.
8. D. P. H. HASSELMAN, *Amer. Ceram. Soc. Bull.* 42 (1970) 1033.
9. W. M. ROHSANOW and H. Y. CHOI, "Heat, Mass and Momentum Transfer" (Prentice-Hall, Englewood Cliffs, New Jersey, 1961) p. 212 et. seq.
10. R. W. DAVIDGE and G. TAPPIN, *Trans. Brit. Ceram. Soc.* 66 (1967) 405.
11. S. S. MANSON and R. W. SMITH, *Trans. A.S.M.E.* 78 (1956) 533.
12. G. J. MAY, *J. Power Sources* 3 (1978) 1.
13. G. J. MAY and C. M. B. HENDERSON, *J. Mater. Sci.* 14 (1979) 1229.
14. G. D. MILES and F. J. P. CLARKE, *Phil. Mag.* 6 (1961) 1449.
15. P. STANLEY and F. S. CHAN, "Thermal Stresses in Severe Environments", edited by D. P. H. Hasselman and R. A. Heller (Plenum, New York, 1980) pp. 61–80.
16. W. H. KOHL, "Handbook of Materials and Techniques for Vacuum Devices" (Reinhold, New York, 1967).
17. W. R. MORGAN, *J. Amer. Ceram. Soc.* 14 (1931) 913.
18. R. STEVENS, *J. Mater. Sci.* 9 (1974) 934.

Received 10 January
and accepted 24 January 1984